Journal of Alloys and Compounds 505 (2010) 568–572

Contents lists available at ScienceDirect

Journal of Alloys and Compounds

journal homepage: www.elsevier.com/locate/jallcom

Synthesis and characterization of $BaTiO_3$ nanoparticles in oxygen atmosphere

S. Fuentes[a,f,*], R.A. Zárate[b], E. Chávez[b], P. Muñoz[c,f], M. Ayala[c], R. Espinoza-González[d], P. Leyton[e]

[a] Departamento de Química y Farmacia, Facultad de Ciencias, Universidad Católica del Norte, Casilla 1280, Antofagasta, Chile
[b] Departamento de Física, Facultad de Ciencias, Universidad Católica del Norte, Casilla 1280, Antofagasta, Chile
[c] Departamento de Química, Facultad de Ciencias, Universidad Católica del Norte, Casilla 1280, Antofagasta, Chile
[d] Departamento de Ciencia de los Materiales, Facultad de Ciencias Físicas y Matemáticas, Universidad de Chile, Av. Tupper 2069, Santiago, Chile
[e] Laboratorio de Fotofísica y Espectroscopia Molecular, Instituto de Química, Pontificia Universidad Católica de Valparaíso, Av. Brasil 2950, Valparaíso, Chile
[f] Center for the Development of Nanoscience and Nanotechnology, CEDENNA, Santiago, Chile

ARTICLE INFO

Article history:
Received 12 January 2010
Received in revised form 10 June 2010
Accepted 11 June 2010
Available online 23 June 2010

Keywords:
Sol–gel process
Nanostructures
Barium compounds
Ferroelectric materials

ABSTRACT

A new synthesis route to obtain high-purity barium titanate, $BaTiO_3$, using the sol–gel-hydrothermal reaction of $TiCl_4$ and a $BaCl_2$ solution in an oxygen atmosphere has been developed. The synthesized $BaTiO_3$ nanoparticles are nearly spherical. Their grain sizes are determined by the reaction temperature, reaching values as low as 50 nm when the particles are synthesized at 200 °C; interestingly even those particles with the smallest grain sizes displayed a ferroelectric behavior as characterized by a polarization hysteresis loop. The microstructure and composition of the as-synthesized samples were investigated by X-ray diffraction (XRD), high-resolution TEM (HRTEM), Raman spectroscopy, atomic force microscopy (AFM) and energy-dispersive X-ray spectroscopy (EDS).

1. Introduction

Barium titanate (BT) has been one of the best known and widely used materials for electric ceramics due to its excellent dielectric, piezoelectric, pyroelectric and ferroelectric properties [1–6]. $BaTiO_3$ is mainly used in multilayer ceramic capacitors (MLCCs), sensors and actuators, electro-optic devices, thermistors, integral capacitors in printed circuit boards (PCBs), temperature–humidity gas sensors, memory applications, etc. However, it is difficult to develop a dielectric layer of less than 10 μm with large capacitance, which is a major requirement for MLCC miniaturization and electronic/microelectronic devices [7]. Therefore, in order to get further compactness is strongly needed to synthesize BT powders with particle sizes smaller than 100 nm and with high dielectric constant.

The controllable preparation of crystalline BT particles and thin films has been extensively investigated since BT dielectric and ferroelectric properties strongly depend on its microstructure (crystallinity and grain size) [8–10]. Indeed, it is known that the improved BT microstructure has a direct impact on the increasing of electronic devices performance. The traditional preparation methods of perovskite-type powders are performed by solid-state reactions at high temperatures, usually higher than 1000 °C, and under specific pressure and pH conditions [11,12]. Several techniques are available for synthesizing fine BT powders; these include sol–gel [13,14], microwave [15], hydrothermal methods [16–18], and sputtering [19]. In recent years some new methods have been introduced to make porous $BaTiO_3$ too. These methods include the development of soft-chemistry routes to produce nanoparticles or specially shaped materials, such as one-dimensional nanowires [20,21], sonochemical methods to prepare size-tunable BT crystals [22], and the introduction of biosynthesis methods to prepare BaTiO3 nanopowders [23]. Among these synthetic methods, hydrothermal or chemical reaction methods are of great interest, because they are safe and environmentally friendly. The syntheses are performed at moderate temperatures, i.e. ~200 °C, and they are effective for creating novel architectures or hierarchical structures based on nanocrystals [24]. To the best of our knowledge, the influence of the atmosphere in the use of hydrothermal methods to prepare BT has not been yet reported in the literature.

In this paper we report a new route to direct synthesize nanocrystalline $BaTiO_3$ powder using $TiCl_4$ and $BaCl_2$ as starting materials. The route used is a sol–gel-hydrothermal method under oxygen atmosphere, which has allowed us to obtain tetragonal BT and particle sizes of less than 100 nm.

* Corresponding author at: Departamento de Química y Farmacia, Facultad de Ciencias, Universidad Católica del Norte, Av. Angamos 0610, Casilla 1280, Antofagasta, Chile. Tel.: +56 55 355517; fax: +56 55 355521.
E-mail address: sfuentes@ucn.cl (S. Fuentes).

0925-8388/$ – see front matter © 2010 Elsevier B.V. All rights reserved.
doi:10.1016/j.jallcom.2010.06.074

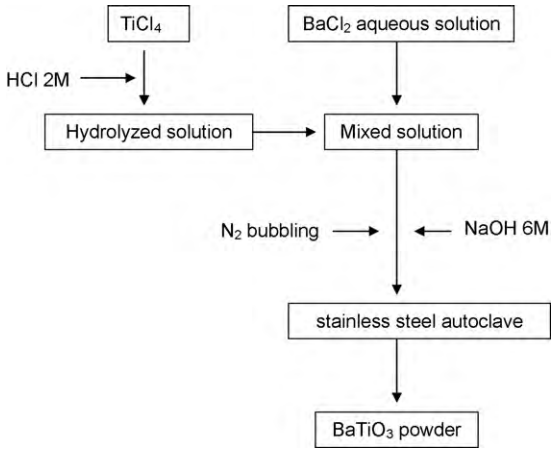

Scheme 1. The reaction procedure of synthesizing $BaTiO_3$ nanoparticles.

2. Experimental

In a typical procedure, 1.1 ml of $TiCl_4$ was diluted in 2.3 ml of HCl 2 M to form a yellowish solution, and 2.4 g $BaCl_2{\cdot}2H_2O$ was dissolved in 15 ml of deionized water. The two solutions were mixed to form a barium titanium solution. Under stirring and N_2 bubbling, 13 ml of NaOH 6 M was added to the barium titanium solution, which produce a homogeneous colloidal barium titanium slurry. The colloidal mixed solution was transferred into a 500 ml Teflon-lined stainless autoclave and heated at different temperatures (70–220 °C) during 3 h. The experiments were developed under two different atmospheres: Oxygen (Met 1) and air (Met 2); Met 2 is the conventional methodology. In Met 1 the autoclave was sealed, evacuated and refilled with pure oxygen. The pressure was controlled during the experience at a fixed value of 60 bar (the reaction procedure for Met 1 is illustrated in Scheme 1). In Met 2 the autoclave was sealed with the normal air inside, and during the experience the pressure reached the equilibrium value for each reaction temperature. At the end of the reaction, the autoclave was naturally cooled to room temperature. The as-formed solid white powder attached to the bottom and inner wall of the Teflon container was collected, centrifuged, washed with distilled water and ethanol to remove remaining ions, and dried at 60 °C for 6 h in vacuum.

The samples obtained were analyzed by XRD using a Siemens D5000 diffractometer with Cu Kα radiation (40 kV, 30 mA). The morphology of the samples was observed using a low vacuum scanning electron microscope (LV-SEM, JSM-6360LV) equipped with an EDS detector. Transmission electron microscopy (TEM) studies were performed in a Tencai F20 FEG-TEM operated at 200 kV, equipped with an EDS detector. The TEM samples were ultrasonically dispersed in isopropanol and then collected in a carbon grid. The Raman spectra were recorded on a WITEC model CRC200, using a 5.5 mW laser with a wavelength of 514.5 nm. The AFM images were obtained by the same equipment.

3. Results and discussion

Fig. 1 shows the XRD patterns of powders obtained at different reaction temperatures using the Met 1 procedure. All products exhibited similar XRD patterns and presented an increase of the crystallinity with the reaction temperature.

The exhibited peaks can be indexed as cubic lattice (space group *Pm*3*m*) of $BaTiO_3$ and the calculated lattice constants are in good agreement with the tabulated values (JCPDS cards No. 31-0174). The inset image shows the detailed XRD patterns of the BT (2 0 0) reflection. Only a single diffraction peak at $2\theta = 45°$ is observed with no split, as it would be expected if the tetragonal phase would be present. This implies that the particles are apparently stabilized in the cubic form at room temperature. Chen et al. reported that the reaction temperature has a remarkable effect on the crystal structure inducing a position change of the (2 2 0) reflection plane [18]. The present results indicate that when the reaction temperature increases from 80 to 200 °C, the (2 2 1) peak shifts from $2\theta = 55.3°$ to $2\theta = 56.1°$ [25].

The crystallite size was estimated from the BT(1 1 0) reflection as measured by XRD and using the Debye–Scherrer equation. The FWHM of the sample synthesized at 220 °C was 0.24845°, corresponding to a crystallite size of ~50 nm. The comparison of the crystallite size of BT powders prepared by Met 1 and by Met 2 is presented in Table 1. All the samples prepared with oxygen (Met 1) had a crystallite size in the range of 50 nm, while the samples prepared by Met 2 exhibited larger values, i.e. ~100 nm).

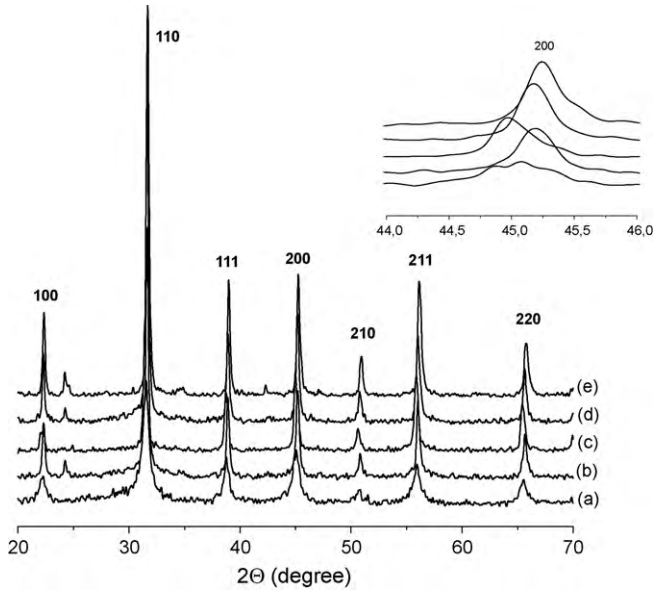

Fig. 1. XRD patterns of the product obtained with 3 h at different reaction temperatures: (a) 80, (b) 120, (c) 160, (d) 200 and (e) 220 °C. The inset shows the XRD patterns in the 2 °C region of 44 and 46°.

In contrast to XRD technique, Raman spectroscopy is a highly sensitive technique to probe the local structure of $BaTiO_3$ samples. $BaTiO_3$ single crystals at room temperature have a tetragonal perovskite structure (space group *P*4*mm*) with one formula unit per unit cell. Only below the Curie point, near 120 °C, does $BaTiO_3$ become ferroelectric. In the interval 120–1460 °C $BaTiO_3$ monocrystals take the paraelectric cubic perovskite structure (space group *Pm*3*m*). The vibrational modes in the cubic structure are 3*F*1*u* + *F*2*u* [26]. *F*2*u* and *F*1*u* are not Raman active modes because the first-order Raman scattering is symmetrically forbidden in bulk $BaTiO_3$. The lowered unit cell symmetry of the tetragonal $BaTiO_3$ causes that each of the three *F*1*u* modes splits into A1 + E, and that the *F*2*u* mode splits into B1 + E. The vibrational modes in this structure are 3A + 4E + B1. Therefore, the tetragonal phase can be distinguished displaying Raman active modes by vibrational spectroscopy.

The Raman spectra of the $BaTiO_3$ nanoparticles prepared by Met 1 are presented in Fig. 2. Raman active modes attributed to tetragonal BT do not clearly appear for samples prepared at temperatures under 160 °C (curves a and b), and only weak plasmon peaks are observed. This confirms the cubic phase of the nanoparticles obtained at these reaction temperatures.

Table 1
Crystalline size calculated by Scherrer formula for $BaTiO_3$ with (Met 1) and without (Met 2) oxygen atmosphere.

Temperature (°C)	Crystal size (nm)	
	Met 1	Met 2
80	55.23	93.45
120	55.65	92.65
160	51.23	83.55
200	49.45	85.88
220	49.54	72.54

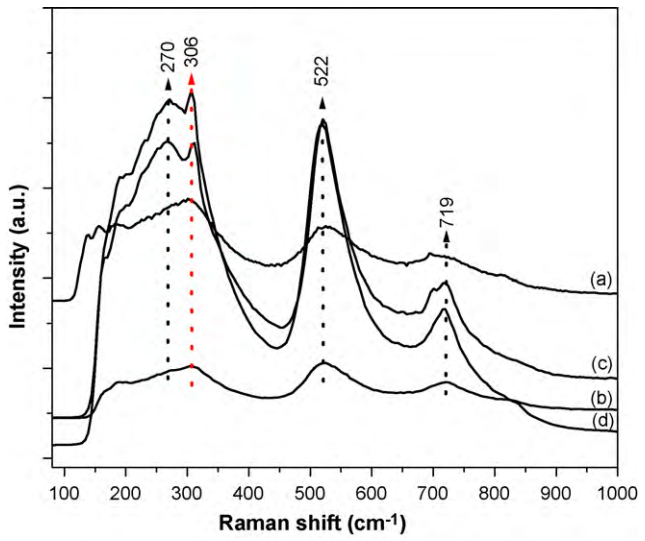

Fig. 2. Raman spectra of the product obtained at different reaction temperatures: (a) 120, (b) 160, (c) 200 and (d) 220 °C.

On the other hand, Raman results of samples prepared at temperatures over 200 °C (curves c and d) showed sharp bands around 175 cm^{-1} [A1(TO), E(LO)] and 305 cm^{-1} [B1, E(TO + LO)] and broad bands around 265 cm^{-1} [A1(TO)], 520 cm^{-1} [A1, E(TO)], and 720 cm^{-1} [A1, E(LO)]. These peaks are characteristic active modes of the tetragonal phase of $BaTiO_3$ [26], which suggest a transition from cubic to pseudotetragonal phase with the increase of reaction temperature. The appearance of strong Raman peaks near 305 cm^{-1} (B1 mode), that corresponds to tetragonal BT phase is contradictory with the cubic symmetry observed by XRD analysis, for which no first-order Raman activity is expected. Busca et al. [27] reported a distortion of the TiO_6 octahedron in the cubic BT phase inducing a pseudotetragonality of the cubic phase. This could explain the significantly lower symmetry with respect to a cubic perovskite structure, similar to that of the tetragonal $BaTiO_3$.

It is believed that there is a critical crystallite size for the BT for stabilizing the cubic or the tetragonal phase [9]. This means that if the crystallite size is lower than the critical value, the phase should be cubic. In the particular case of bulk BT, the body retains its ferroelectricity unless the average grain size is less than 50 nm [9]. In the present paper we report that is possible to obtain BT powders with particle size about 50 nm that presents a pseudotetragonal crystallographic structure, i.e. with the *a*, *b* and *c* equal axes but the titanium atoms are slightly displaced from the center of cubic structure by about 6 pm [28]. This crystal structure clearly exhibited ferroelectric behavior as confirmed by hysteresis loops.

The morphology of the samples was analyzed by atomic force microscopy (AFM) using acoustic or tapping mode. The particles have almost spherical shape, as shown in Fig. 3. The average particle size estimated from AFM images was ~70 nm for the sample treated at 220 °C and prepared by Met 1. It is important to note that the average particle size estimated by AFM images is larger than the size calculated by the Debye–Scherrer formula [29], pointing out a possible polycrystalline structure in the BT grains.

Transmission electron microscopy (TEM) and high-resolution transmission electron microscopy (HRTEM) images provided an insight into the structure of the BT particles prepared at 220 °C with Met 1, as it is shown in Fig. 4. The bright-field low-magnification TEM image reveals that the BT nanoparticles are nearly spherical with a diameter range of 50–75 nm (see Fig. 4a). This particle size is in good agreement with the calculated value from Debye–Scherer formula, which was about 50 nm (Table 1) and the AFM results. HRTEM image in Fig. 4b, oriented to a (1 1 1) zone axis, shows that the regular spacing of the observed lattice planes was about 0.283 nm, which corresponds to the interplanar distance of the (0 1 1) plane of cubic BT. SAED pattern in Fig. 4c displays a polycrystalline diffraction rings composed of discrete diffraction spots which indicates the polycrystalline nature of the nanoparticles. EDS analysis (Fig. 4d) of the same sample showed only the presence of Ba, Ti and O, with no indication of contamination.

One of principal features of ferroelectric materials is that the spontaneous polarization is reversible, at least partially, through the application of an external electric field. The experimental manifestation is measured by the Hysteresis loop, which is frequently used as a test to demonstrate that a material is ferroelectric [30]. Fig. 5 shows the hysteresis loop measured through a Sawyer–Tower circuit. This circuit consists in two capacitors in series that are connected to a variable potential. One of the capacitors is our sample which is powered compressed as a pill with gold electrodes deposited by sputtering, with an approximated area of about 0.0401 cm^2 and a thickness of about 0.068 cm. This circuit allowed us to estimate the spontaneous and the remnant polarizations and the coercitive field, which were $P_r = 2.2\ \mu C/cm^2$ and $E_c = 32$ kV/cm, respectively.

The oxygen partial pressure plays a crucial role in the BT-nanoparticle formation under hydrothermal conditions. Zhang et al. [31] reported the neutral vacancies formation energies studied by *ab initio* calculations for the $PbTiO_3$ system. Under oxygen-rich conditions, Pb-vacancies are ready to form due to its lowest

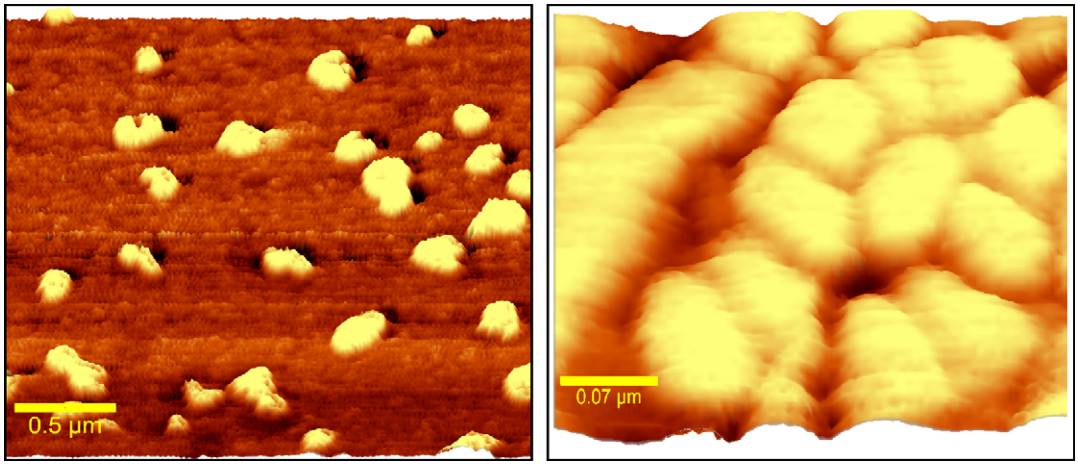

Fig. 3. Acoustic AFM images of $BaTiO_3$ nanoparticles obtained at 220 °C.

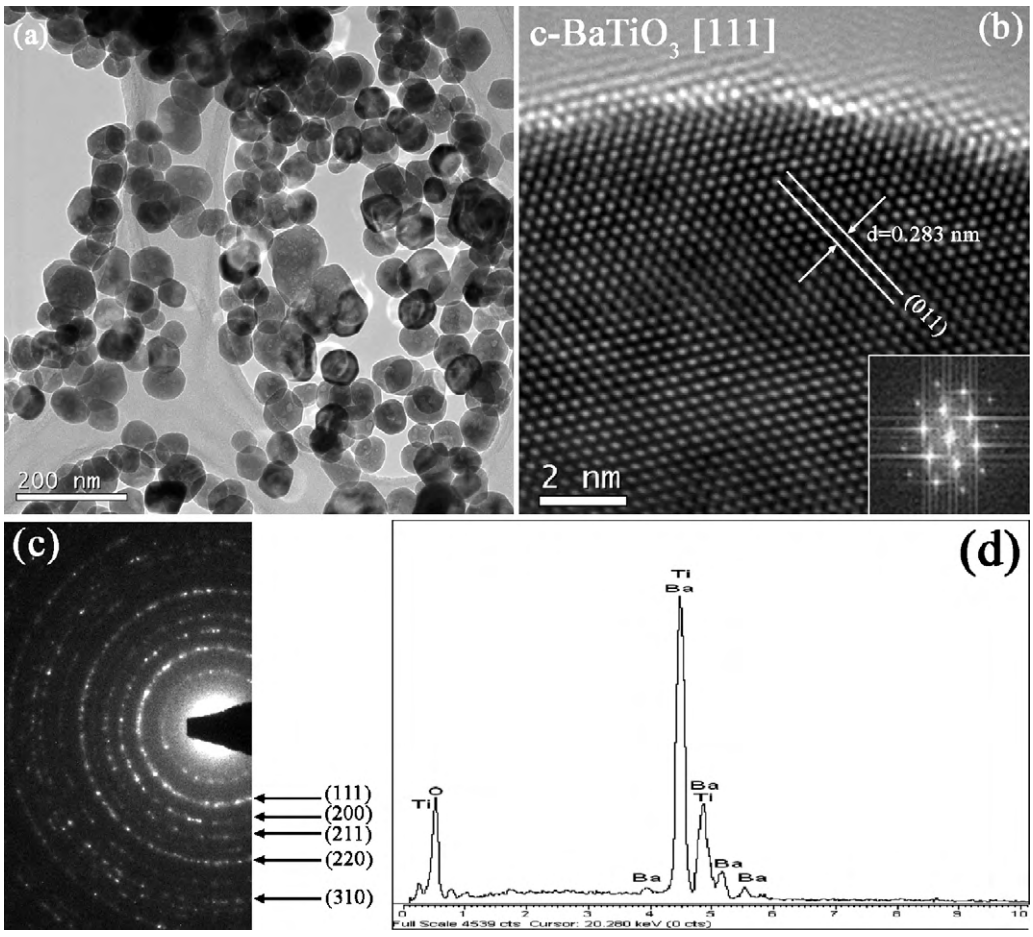

Fig. 4. Morphology and structure of the $BaTiO_3$ nanoparticles obtained at 220 °C. (a) TEM image, (b) HRTEM image, (c) SAED pattern, and (d) corresponding EDX.

formation energy and under oxygen-poor conditions; O-vacancies become more dominant than Pb-vacancies. Under both conditions the vacancies of oxygen bonded with Ti in *z* direction are always easier to form than those bonded with Ti in *x*–*y* plane, thus affecting the ferroelectricity of the crystal.

We think that oxygen partial pressure helps the transition of BT from cubic to pseudotetragonal phase when the reaction temperature is about 200 °C. This is caused by the reduction oxygen vacancies concentration. Furthermore, the decrease of oxygen vacancies after the reaction in oxygen atmosphere will increase the ferroelectric exchange interactions, which are mediated by the oxygen ions, influencing the ferroelectric properties of BT. In the present results it was shown that the oxygen atmosphere can effectively enhance the ferroelectric of $BaTiO_3$ nanoparticles. On the other hand, it is possible that the high pressure does not allow to increase the crystal size because it is favored the nucleation and not the coalescence process. Experiments to isolate this variable are under course.

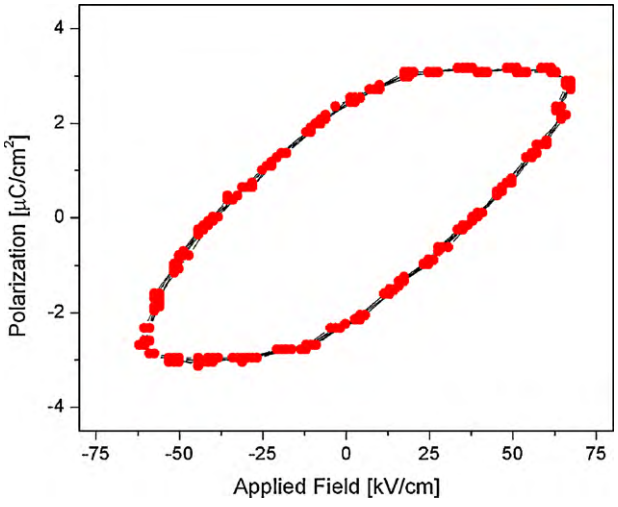

Fig. 5. Room-temperature polarization versus electric field curve of the $BaTiO_3$ nanoparticles obtained at 220 °C.

4. Conclusions

We have successfully synthesized ferroelectric nanocrystallites of BT with grain sizes in the range from 50 to 75 nm by a sol–gel-hydrothermal method under an oxygen partial pressure of 60 bar.

XRD and SAED results suggest that the BT nanoparticles are in cubic phase. The crystallinity of the BT increased with the incorporation of an oxygen partial pressure. On the other hand, the Raman active modes of our samples are similar to the tetragonal phase of BT. The presence of the peak at 305 cm^{-1} confirms the transition of BT from cubic to a pseudotetragonal phase with the increase of the reaction temperature from 80 to 220 °C. The (pseudo)tetragonal domains exhibited a ferroelectric behavior characterized by a spontaneous polarization as detected by the typical hysteresis loop that characterizes ferroelectric materials.

Acknowledgments

This work has been partially financed by FONDECYT grant under contract No. 1080401, Basal Financing Program CONICYT, FB0807 (CEDENNA). The authors thank the Facultad de Ciencias Físicas y Matemáticas of the Universidad de Chile for the use of their analytical equipment (XRD and TEM). R.A.Z. acknowledges FUNDACION ANDES grant under contract No. C-13876. E. Chavez acknowledges to CONICYT under grant 22090805.

References

[1] N. Setter, D. Damjanovic, L. Eng, G. Fox, S. Gevorgian, S. Hong, A. Kingon, H. Kohlstedt, N.Y. Park, G.B. Stephenson, I. Stolitchnov, A.K. Taganstev, D.V. Taylor, T. Yamada, S. Streiffer, J. Appl. Phys. 100 (2006) 051606–051652.
[2] J. Xu, J. Zhai, X. Yao, J. Alloys Compd. 467 (2009) 567–571.
[3] J. Lott, C. Xia, L. Kosnosky, C. Weder, J. Shan, Adv. Mater. 20 (2008) 3649– 3653.
[4] L. Louis, P. Gemeiner, I. Ponomareva, L. Bellauche, G. Geneste, W. Ma, N. Setter, B. Dkhil, Nano Lett. 6 (10) (2010) 1177–1183.
[5] R.V. Mangalam, N. Ray, U. Waghmare, A. Sundaresan, C.N.R. Rao, Solid State Commun. 149 (2009) 1–5.
[6] A. Choudhury, Mater. Chem. Phys. 121 (2010) 280–285.
[7] L. Martin, Y. Chu, R. Ramesh, Mater. Sci. Eng. R (2010), doi:10.1016/j.mser.2010.03.001.
[8] T. Hoshina, S. Wada, Y. Kuroiwa, T. Tsurumi, Appl. Phys. Lett. 93 (2008) 192914–192916.
[9] A. Sundaresan, R. Bhargavi, N. Rangarajan, U. Siddesh, C.N.R. Rao, Phys. Rev. B 74 (2006) 161306–161310.
[10] N. Nuraje, K. Su, A. Haboosheh, J. Samson, E. Manning, N. Yang, H. Matsui, Adv. Mater. 18 (2006) 807–812.
[11] C.-Y. Chang, C.-Y. Huang, Y.-C. Wu, C.-Y. Su, C.-L. Huang, J. Alloys Compd. 495 (2010) 108–112.
[12] W.S. Jung, J.H. Kim, H.T. Kim, D.H. Yoon, Mater. Lett. 64 (2010) 170–172.
[13] S. Yoon, S. Baik, M.G. Kim, N. Shin, I. Kim, J. Am. Ceram. Soc. 90 (2007) 311–314.
[14] R. Kavian, A. Saidi, J. Alloys Compd. 468 (2009) 528–532.
[15] K. Sadhana, T. Krishnaveni, K. Praveena, S. Bharadwaj, S. Murthy, Scripta Mater. 59 (2008) 495–498.
[16] H. Hayashi, T. Noguchi, N.M. Islam, Y. Hakuta, Y. Imai, N. Ueno, J. Cryst. Growth 312 (2010) 1968–1972.
[17] X. Zhu, J. Wang, Z. Zhang, J. Zhu, S. Zhou, Z. Liu, N. Ming, J. Am. Ceram. Soc. 91 (2008) 1002–1008.
[18] C. Chen, Y. Wei, X. Jiao, D. Chen, Mater. Chem. Phys. 110 (2008) 186–191.
[19] Q. Liang, X. Fang-Bi, J. Phys. D: Appl. Phys. 42 (2009) 175508–175514.
[20] C. Fu, W. Cai, L. Zhou, H. Chen, Z. Liu, Appl. Surf. Sci. 255 (2009) 9444–9446.
[21] K.C. Huang, T.C. Huang, W.F. Hsieh, Inorg. Chem. 48 (2009) 9180–9184.
[22] F. Dang, K. Kato, H. Imai, S. Wada, H. Haneda, M. Kuwabara, Ultrason. Sonochem. 17 (2010) 310–314.
[23] A.K. Jhaa, K. Prasad, Colloids Surf. B 75 (2010) 330–334.
[24] S. Adireddy, C. Lin, B. Cao, W. Zhou, G. Caruntu, Chem. Mater. 22 (2010) 1946–1948.
[25] C.T. Xia, E.W. Shi, W.Z. Zhong, J.K. Guo, J. Eur. Ceram. Soc. 15 (1995) 1171–1176.
[26] D. Tenne, X. Xi, J. Am. Ceram. Soc. 91 (2008) 1820–1834.
[27] G. Busca, V. Buscaglia, M. Leoni, P. Nannit, Chem. Mater. 6 (1994) 955–961.
[28] E. Chávez, S. Fuentes, R.A. Zarate, L. Padilla-Campos, Structural analysis of the nanomaterial of $BaTiO_3$, J. Mol. Struct. Submitted for publication.
[29] P. Klug, L.E. Alexander, X-ray Diffraction Procedure, Wiley, New York, 1954.
[30] I. Mayergoyz, G. Bertotti, The Science of Hysteresis, Elsevier, 2005.
[31] Z. Zhang, P. Wu, L. Lu, C. Shu, J. Alloys Compd. 449 (2008) 362–365.